Acta Scientific Gastrointestinal Disorders (ISSN: 2582-1091)

Volume 8 Issue 8 August 2025

Case Report

IgG4-Associated Disease: Difficulties in Early Diagnosis

Mitusheva Elvina Ilnurovna, Saifutdinov Rafik Galimzijanovich* and Mayorova Elena Mikhailonva

Department of Hospital and Ambulatory Therapy, Kazan State Medical Academy for Post degree Education-Branch Campus of the FSBEI FPE RMACPE MOH Russia, Russian Federation

***Corresponding Author:** Saifutdinov Rafik Galimzijanovich, Department of Hospital and Ambulatory Therapy, Kazan State Medical Academy for Post degree Education-Branch Campus of the FSBEI FPE RMACPE MOH Russia, Russian Federation.

Received: July 09, 2025

Published: July 29, 2025

Abstract

The article presents data on IgG4-associated disease. The disease has many different phenotypes, differing in epidemiological, serological data, prognostic outcomes, and effectiveness of therapy. The disease mimics a tumor, infectious and inflammatory disease. The presented clinical case of a 48-year-old patient confirms the difficulties of early diagnosis of the disease. Timely verification of the diagnosis of IgG4-associated disease is of important clinical and prognostic importance.

Keywords: Cholangitis, cholestasis, autoimmune pancreatitis, sclerosing cholangitis, fibrotic disease, Mikulich's disease

Abbreviations

ALT: Alanine Aminotransferase; ASTs: Aspartate Aminotransferase; BBT: Biochemical Blood Test; CRPs: C-Reactive Protein; CT: Computed Tomography; GBT: General Blood Test; IgE: Immunoglobulin E; IgG: Immunoglobulin G; IgG1: Immunoglobulin G1; IgG2: Immunoglobulin G2; IgG4: Immunoglobulin G4; IgG4-AD: IgG4-Assotiated Disease; IgG4-SC: IgG4-Associated Sclerosing Cholangitis; MR: Magnetic Resonance; MRI: Magnetic Resonance Imaging; RES: Rate of Erythrocyte Sedimentation; RNA: Ribonucleic Acid; USI: Ultrasound Investigation

Introduction

The IgG4-related disease was recognized as a single disease only 15 years ago. Since then, awareness of the IgG4-related disease has increased worldwide, and experts are now familiar with most of its clinical manifestations. Lesions of the pancreas and biliary tract, retroperitoneal space/aorta, head and neck, and salivary glands are the most commonly observed phenotypes of the disease, differing in epidemiological features, serological data, and prognostic outcomes. Taking into account the versatility of phenotypic manifestations, IgG4-assotiated disease mimics a tumor, inflammatory, and infectious disease. Histopathology remains the key to diagnosis, as there are no reliable biomarkers.

According to Japanese studies, the incidence of IgG4-AD increased from 0,8 to 3,1 cases per 100.000 people between 2007 and 2016, indicating a rapid increase in the incidence in less than a decade. IgG4-AD usually affects middle-aged and elderly people with a male-to-female ratio of 1,6:1 in head and neck lesions, up to 4:1 in other organs [18].

An inflammatory reaction plays a role in the pathogenesis of the disease, characterized by the appearance of B and T lymphocytes, which accumulate in the foci of the disease and enter into mutually activating antigen-controlled interactions, as well as secrete profibrotic molecules such as interleukin 1b, interleukin 6, interferon γ, transforming growth factor β, platelet-derived growth factor β, homologue lysyl oxidase-2. Fibroblasts are also activated and colla-

gen is produced [1-3]. The abundance of IgG4-positive plasma cells in the affected tissues and fibrosis are characteristic pathological signs of this disease. The final diagnosis of IgG4-AD requires strict clinical and pathological correlation, since the clinical picture, laboratory data, and imaging studies are often insufficient to differentiate between tumor, inflammatory, and infectious disease. Serological data in patients with IgG4-AD are largely non-specific. The erythrocyte sedimentation rate can be increased to a moderate degree. C-reactive protein is usually normal, with the exception of some clinical manifestations, such as lesions of the retroperitoneal space and aorta, in which a slight increase may occur. A marked increase in acute phase proteins should be of concern in terms of infectious of inflammatory conditions that mimic IgG4-AD. Peripheral blood eosinophilia and elevated serum IgE concentrations occur in almost 30% of patients with IgG4-AD. Some patients have a low titer of antinuclear antibodies and a positive rheumatoid factor. An increase in serum IgG4 levels is observed in 55-97% of cases, especially in patients of Asian origin.

In a meta-analysis of nine case-control studies involving 1,235 patients with IgG4-AD and 5,696 controls, the cutoff value for serum IgG4 was 1.35 g/L to 1.44 g/L, with a sensitivity of 87.2% (95% CI 85.2% to 89.0%) and a specificity of 82.6% (95% CI 81.6% to 83.6%). When a twofold increase above the upper limit of the normal range (2.70-2.80 g/L) was used as the threshold value, the total sensitivity and specificity were 63% (60.0-66.0%) and 94.8% (94.1-95.4%), respectively [4]. An increase in the serum level of IgG4 is informative for initial screening, but it has low diagnostic value because it can be observed in a wide range of tumor, infectious, and autoimmune diseases [5-8]. In addition, measuring IgG4 levels in blood serum is not without analytical errors. Most laboratories around the world quantify IgG4 concentrations either by turbidimetry or by nephelometry, with the former method producing spuriously normal IgG4 values in the case of excess antigen ("prozone phenomenon") [9,10].

Several new serological and cellular biomarkers have been proposed and are awaiting confirmation in large prospective multicenter studies. It has been shown that an increased ratio of serum IgG4 to total IgG (>10%) or IgG1 (>24%) improves diagnostic specificity, especially when the concentration of IgG4 is only slightly elevated [11]. Quantitative polymerase chain reaction, used to calculate the ratio of IgG4:IgG RNA in peripheral blood, appeared to accurately distinguish IgG4-associated cholangitis from malignant neoplasms of the hepatobiliary system and inflammatory processes with a sensitivity of 94% and a specificity of 99% [12]. An increase in the serum concentration of IgG2 above 5.3 g/L provided a sensitivity of 80% and a specificity of 91.7% for the diagnosis of orbital IgG4-AD [13].

(Table 1)

According to research, men are more susceptible to IgG4-AD. Asian patients have a higher risk of developing IgG4-AD in the form of head and neck lesions. Additionally, patients with head and neck lesions are more likely to have atopic manifestations. Patients with Mikulicz's disease/systemic disease have a higher number of affected organs and higher serum concentrations of IgG4 and IgE. Phenotypes with retroperitoneal and head and neck involvement seem to be more prone to fibrotic outcomes than other phenotypes, making them more difficult to treat [18].

IgG4-AD is well-treated and responds quickly to glucocorticoids, but if it is not diagnosed in time, it can lead to terminal organ failure and even death. Glucocorticoids are recommended as first-line therapy to achieve remission. Treatment with glucocorticoids should be started at a dose of 0.6-0.8 mg/kg/day orally for 1 month to induce remission, but the initial dose of glucocorticoids may be adjusted. This adjustment should be based on body weight in the case of an extremely aggressive disease (initial doses of >40 mg/day are used) or in elderly patients with very mild symptoms (doses of less than 20 mg/day are used).

Despite the effectiveness of glucocorticoids, approximately one-third of patients experience a relapse of the disease after reducing the dose of the medication, which requires repeated induction therapy [14]. For this purpose, the dose of glucocorticoids is usually increased and then gradually reduced over time. The relapse may occur in the same organ that was initially affected, or, interestingly, in an organ that was not previously involved [14,15]. Relapse is more common in patients who have not previously received glucocorti-

The phenotype	Pancreato-biliary	Retroperitoneal/Aortitis	Head and neck	Mikulicz's disease/ Systemic disease
	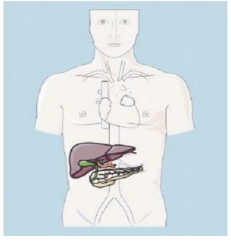	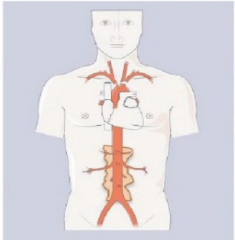	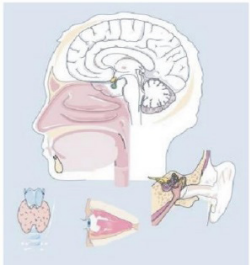	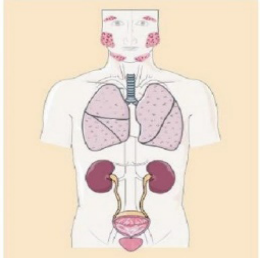
Diagnostics	Male White race Average age IgG4 ↑↑ IgE ↑	Male White race Average age IgG4 ↑/ = RES/CRP ↑	Female Asian race Young age Atopic history IgG4 ↑↑	Male - Average age IgG4 ↑↑↑ IgE ↑
Management tactics	A good response to glucocorticoids	Fibrosing disease Refractory to treatment	Fibrosing disease Refractory to treatment	A good response to glucocorticoids
Organ damage	Pancreas – type 2 diabetes, malabsorption syndrome, exocrine pancreatic insufficiency. Biliary tract and liver: sclerosing cholangitis, bacterial cholangitis, liver failure.	Pericardium – constrictive pericarditis. Heart – damage to the coronary arteries. Aorta: inflammation of the thoracic and abdominal aorta with the development of aneurysms. Retroperitoneum: atrophy of the kidneys, damage to the kidneys up to the development of hydronephrosis, chronic abdominal pain syndrome. Mediastinum: compression of nearby organs.	The eyeball: exophthalmos, loss of vision, diplopia. The meninges: cranial nerve paralysis. The skull bones and sinuses: chronic sinusitis, midline destructive lesions, anosmia. The thyroid and parathyroid glands: hypothyroidism, hypopituitarism.	Lacrimal glands: dryness. Salivary glands: dryness. Pancreas – type 2 diabetes, malabsorption syndrome, exocrine pancreatic insufficiency. Lungs: pulmonary fibrosis and interstitial lung disease. Pleura: effusion and thickening. Kidneys: renal failure, glomerulonephritis.

Table 1: Characteristics of IgG4-associated disease phenotypes [18].

coids (about 40%) than in patients who have previously received glucocorticoid therapy (about 25%). Some experts recommend maintenance therapy with glucocorticoids at doses of ≤10 mg/day (equivalent to 2.5-10 mg/day of prednisolone) for 12 months. In some Japanese centers, low-dose (5 mg) prednisolone therapy is continued for 3 years [16] or even longer [17]. At least three treatment regimens are used for relapse: (a) high-dose glucocorticoids followed by low-dose glucocorticoids or steroid-sparing drugs; (b) high-dose glucocorticoids without maintenance therapy; or (c) induction therapy with rituximab followed by maintenance therapy with or without rituximab. Since glucocorticosteroids are highly effective in inducing remission (>95%), it is advisable to repeat the course of high-dose glucocorticoids if the patient tolerates it. In patients who are resistant to or intolerant of high-dose glucocor-

ticoids, rituximab is indicated for maintaining remission or in the absence of response to immunosuppressive therapy. The drug is administered (375 mg/m2 of body surface area) once a week for 4 weeks, and then once every 2-3 months, or as two 1000 mg infusions separated by 15 days every 6 months. In addition to rituximab, other cytostatics can be used: thiopurines (azathioprine and 6-mercaptopurine), mycophenolate mofetil, methotrexate, or calcineurin inhibitors (tacrolimus and cyclosporine A).

A clinical case of a patient with IgG4-AD is presented.

Patient M., 48 years old, was admitted to the Gastroenterology Department of City Clinical Hospital №12 in Kazan on July 20, 2022, with complaints of severe general weakness, itchy skin, and weight loss of 10 kg over a period of 1 year. Her appetite was preserved.

Anamnesis morbi: She has been considered ill since 2020, when she was treated for New Coronavirus Infection (laboratory-confirmed) from 03.12.20 to 23.12.20. She was treated with antiviral medications and paracetamol. On 21.06.2021, she received the Sputnik-V vaccine for New Coronavirus Infection, and 21 days later, she received the second dose of the vaccine. 1 week after vaccination, the proximal phalanx of the IV finger of the right hand swelled, and she consulted a district therapist. As a result of the examination, she was diagnosed with anemia, elevated alkaline phosphatase, and an enlarged liver on ultrasound. She took Heptor. She noticed that she started losing weight in March 2021. Around the beginning of November 2021, she developed skin itching, leading to her hospitalization in the Gastroenterology Department of City Clinical Hospital №12.

From 03.11.21 to 18.11.21, he received inpatient treatment at the Gastroenterology Department of City Clinical Hospital №12 with the following diagnosis: Unspecified hepatitis with cholestasis syndrome (debut of primary biliary cholangitis?). Chronic atrophic gastritis. Hypomotility gallbladder dysfunction. Colorectal dyskinesia. Treatment: Remaxol, Heptral, Ursosan, and Rebagit. After discharge, she continued to take Ursosan 750 mg/day and Rebagit 100 mg x 3 times a day. She was recommended to undergo additional tests for autoantibodies to primary biliary cholangitis, autoimmune hepatitis, and primary sclerosing cholangitis.

In January 2022, there was a severe attack of abdominal pain, and the patient reported that her abdomen had increased in size. Five to six days later, she consulted a local physician, and the city's emergency medical services were called. She was admitted to the emergency surgery department of City Clinic Hospital №7. An abdominal ultrasound revealed a significant amount of free fluid in the abdominal cavity (ascites), and she was recommended for hospitalization in a gastroenterology or general medicine department. However, due to the challenges of providing inpatient treatment for gastroenterological conditions in the context of COVID-19, she was not admitted to the hospital. At home, I took diuretics, Ursosan 1000 mg per day, and Duspatalin.

During the next control of tests in March 2022, the district therapist again identified cholestasis, accelerated RES, sent for hospitalization in City Clinic Hospital №12.

From 28.03.22 to 08.04.22 inpatient treatment in the gastroenterology department of City Clinic Hospital №12 with the diagnosis: Hepatitis of unspecified genesis with cholestasis syndrome. The debut of cholestatic liver disease? Hepatosplenomegaly. Mild anemia. Colorectal dyskinesia. Syndrome of accelerated RES. Consulted by a gynecologist, endocrinologist, surgeon. Treatment: Remaxol, Geptral, Ursosan, Duphalac, Pentoxifylline. Recommended further examination: IgG4 serum, magnetic resonance cholangiopancreatography. After discharge, she took Ursosan 2 capsules x 3 times a day (1500 mg/day).

After the next control of tests in July 2022, the district therapist gave a referral for hospitalization in the gastroenterological department of City Clinic Hospital №12.

Hospitalized on 20.07.2022 in the gastroenterological department of City Clinic Hospital №12.

Objectively: The patient's condition is of moderate severity. The patient's consciousness is clear. The patient is asthenic and lethargic. The patient's height is 164 cm, and her weight is 54 kg. The patient's skin is pale. The patient's mucous membranes are icteric. The patient's small posterior cervical lymph nodes are palpable on both sides. The patient's breathing is vesicular, and there are no wheezing sounds. The patient's respiratory rate is 16 breaths per minute. The heart sounds are rhythmic, and the blood pressure is 120/70 mmHg. The heart rate is 88 beats per minute. The tongue has a white-yellow coating on the edges. The abdomen is soft and painless on palpation. The liver is enlarged, measuring 11x10x9 cm according to Kurlov, and the spleen is enlarged, measuring 10x6.5 cm. The Pasternak sign is negative on both sides.

Laboratory research data

GBT	03.11.21	12.11.21	15.11.21	19.12.21	04.04.22	19.07.22	20.07.23
Leycocytes, x 10^9/l (4 - 9 x10^9/l)	4,4	4,7	5,3	5,7	4,4	8,4	4,2
Erythrocytes, x10^{12}/l (3,7 - 4,7 x10^{12}/l)	3,5	3,9	4,4	3,73	3,6	4,07	3,84
Hemoglobin, g/l (120-140 г/л)	98	111	120	112	107	102	109
RES, mm/h (2 - 15 mm/h)	21	54	54	6	70	56	50
Platelets, x 10^9/l (180 - 320 x 10^9/l)	163	180	180	165	141	107	127
Segmented neutrophils, % (47 - 72%)	47	42	42	46	50	54	43
Band-shaped neutrophils, % (1 - 6%)	2	2	2	0	2	3	0
Lymphocytes, % (18 - 40 %)	38	44	44	41	38	30	47
Eosinophils, % (0 - 5%)	0	4	4	4	4	4	1
Basophils, % (0 - 1%)	0		0	0	0	0	0
Monocytes, % (2 - 9 %)	7	8	8	9	6	9	9

Table 2: Dynamics of a complete blood count.

BBT	29.10.21	03.11.21	09.11.21	19.12.21	29.03.22	12.07.22	20.07.22
Total bilirubin, µmol/L (3,4 - 17,1 µmol/L)	24,1	32,2	25,5	31,2	21,0	16,3	23,6
Direct bilirubin, µmol/L (0 - 3.4 µmol/L)	16,5	9,7	10,0	17,9	8,3	8,5	10,4
Indirect bilirubin, µmol/L (3.4 - 13.7 µmol/L)	7,6	22,5	15,5		12,7		13,2
ALT, U/l (0 - 35 U/l)	70	77	44	49	41	45	104
AST, U/l (0 - 32 U/l)	98,4	92	65	78	63	70	64
GGT, U/l (0 - 38 U/l)			804,5		686,5	688,4	616
Alkaline phosphatase, U/L (30 - 120 U/L)	1937,1	1587	1623		1663	1270	1539
Total protein, g/l (65 - 84 g/l)		78		84	86	84	84
Albumin, g/l (35 - 50 g/l)		35,9				42	
Glucose, mmol/L (3.85 - 5.83 mmol/L)	6,12	5,2					
CRP, mg/L (0 - 0.5 mg/L)	12						4
Rheumatoid factor, IU/ml (0 - 14 IU/ml)	8,2						
Cholesterol, mmol/L (3.0 - 6.0 mmol/L)	7,51						6,6
Alpha-amylase, IU/l (25 - 125 IU/ml)							82
Prothrombin, % (54.7 - 123.7%)			83,3		86,5		
Gamma-globulin, % (11.1 - 18.8%)					24,6	21,5	26,7

Table 3: Dynamics of biochemical blood analysis.

According to laboratory tests, an immune-inflammatory syndrome was detected (accelerated erythrocyte sedimentation rate, increased C-reactive protein, and hypergammaglobulinemia), as well as mild cytolysis (increased ALT to 1.5-2 normal values and AST to 2 normal values), and severe cholestasis (increased direct bilirubin and alkaline phosphatase to 10-12 normal values and gamma-glutamyl transpeptidase to 13-16 normal values).

USI of the abdominal cavity	17.12.21	05.01.22	10.03.22	09.07.22	27.07.22
Liver	126x72 mm, the contours are smooth, clear, the structure is diffusely heterogeneous, iso-hyperechoic with periportal fibrous seals, the vascular pattern is clear, V.portae 9 mm. In the projection of the gate, multiple lymph nodes are determined by the sizes of 13x9 mm, 16x8 mm, along the course of the celiac trunk, lymph nodes 13x7 mm, up to 21x10 mm.	137x62 mm, the contours are smooth and clear, hyperechoic, heterogeneous, with diffuse steatosis	157x89 mm, the contours are smooth and clear, the structure is homogeneous and isoechoic, and the vascular pattern is unchanged	156x89x28 mm, diffuse-heterogeneous with fibrous changes, hyperechoic, vascular pattern moderately weakened, V.portae 12 mm. LSC 18.5 cm/sec. In the projection of the liver gate, a lymph node 14x7 mm is visualized. Along the course of the celiac trunk, lymph nodes up to 15x7 mm are determined and para-aortally at the L1-L2 level, lymph nodes up to 16x7 mm.	137x31x31 mm, diffuse-heterogeneous with fibrotic changes, iso-hyperechoic, vascular pattern weakened, V.portae 11 mm. LSC 15.6 cm/sec, slightly reduced. The liver veins are not dilated. Lymph nodes are detected in the projection of the liver gate and along the celiac trunk, with a maximum size of 12x7 mm.
Gallbladder	53x12 mm, with a bend in the neck. The walls are not altered up to 3 mm, and there are wall-attached inclusions up to 4 mm in diameter. The content is homogeneous, and there are no calculi. The choledoch is 4 mm.	87x18 mm, kinks in the body and neck, the walls are hyperechoic, the content is heterogeneous, no stones are visible, and the choledoch is 5 mm.	60x13 mm, the walls are not thickened, the content is homogeneous, and the choledoch is 4 mm	70x17 mm, with a kink in the neck area, the walls are hyperechoic up to 2 mm thick, there is a 3 mm diameter wall inclusion with no blood flow, the content is homogeneous, there are no calculi, and the choledoch is 5 mm.	67x18 mm, with a bend in the neck. The walls are hyperechoic up to 2.5 mm, and there are wall-attached inclusions up to 3 mm in diameter. The content is heterogeneous, and there are no calculi. The choledoch is 4 mm.
Pancreas	Head 21 mm, body 11 mm, tail 13 mm, structure is homogeneous, contours are smooth, clear, hyperechoic.	Head 33 mm, body 14 mm, tail 18 mm, contours are smooth, borders are clear, hyperechoic, homogeneous.	Head 26 mm, body 11 mm, tail 15 mm, contours are smooth, clear, hyperechoic, homogeneous	Head 25 mm, body 9 mm, tail 13 mm, contours are smooth, clear, hyperechoic, heterogeneous, in the projection of the body the cyst is 5.8 mm in diameter, at the transition point of the body to the tail the cyst is 5 mm in diameter.	the structure is heterogeneous, in the projection of the tail of the cyst with a diameter of 6.8 mm and dimensions of 10x8 mm. The contours are smooth, clear, hyperechoic. Head 23 mm, body 11 mm, tail 18 mm. Wirsung's duct is not dilated 1.5 mm.

Spleen	not enlarged 125x67x81 mm. The structure is homogeneous, the echogenicity is increased, v.lienalis is not dilated 8.4 mm.		133x54 mm, the contours are even, the structure is homogeneous, and the echogenicity is unchanged	enlarged 144x65x108 mm, area 82 cm sq, uniform, v.lienalis not expanded by 7 mm.	enlarged 120x76x94 mm. The structure is homogeneous, the echogenicity is reduced, and the v.lienalis is not dilated by 7 mm.
Conclusion	Signs of moderate diffuse fibrotic changes in the liver (more data for hepatitis), curvature and polyps of the gallbladder, and moderate diffuse changes in the pancreas, mild splenomegaly, focal formation in the spleen, and lymphadenopathy of the intra-abdominal lymph nodes	At the time of examination, free fluid is visualized in the abdominal cavity in large quantities (ascites). Signs of changes in the structure of the liver parenchyma, pancreas, and deformation of the gallbladder.	signs of hepatosplenomegaly	signs of diffuse fibrotic changes in the liver, cirrhosis cannot be ruled out, hepatosplenomegaly, curvature and polyps of the gallbladder, pancreatic cysts, diffuse changes in the pancreas, and lymphadenopathy of the abdominal and retroperitoneal lymph nodes.	signs of diffuse fibrotic changes in the liver, cirrhosis, cholelithiasis, pancreatic cysts, diffuse changes in the pancreas, splenomegaly, and intra-abdominal lymphadenopathy.

Table 4: Dynamics of ultrasonic changes.

According to the ultrasound, lymphadenopathy of intra-abdominal lymph nodes, para-aortic, as well as lymphadenopathy of lymph nodes around the celiac trunk, splenomegaly was diagnosed. Multiple parietal inclusions in the wall of the gallbladder were revealed. The presence of free fluid in the abdominal cavity was detected once.

Autoantibodies (AT):	**21.11.21**	**26.04.22**	**25.06.22**	**30.06.22**	**25.07.23**
AT to mitochondria (AMA-M2)	negative		negative	negative	negative
AT to the liver antigen SP-100	negative		negative	negative	negative
AT to the liver antigen GP-210	negative		negative	negative	negative
AT to soluble liver antigen (SLA/LP)	negative		negative	negative	negative
AT to liver and kidney microsomes (LKM-1)	negative		negative	negative	negative
AT to cytosolic antigen (LC-1)	negative		negative	negative	negative
AT to f-actin	negative		negative	negative	
AT to actinin	negative		negative		
AT to tropomyosin	negative		negative		
IgG4, g/l (0,1 - 1,35)		1,35			2,22
Antineutrophilic cytoplasmic antibodies (ANCA)		negative	negative		
Anti-sp100	negative	negative		negative	negative
Anti-gp210	negative	negative	negative		negative

AT IgG to M2-3E			negative	negative	negative
AT IgG to the mitochondria (AMA-M2)				negative	negative
AT towards double stranded DNA (dsDNA), IgG				negative	negative
AT IgG to antigen nRNP/Sm				negative	negative
AT IgG to antigen SS-A (SS-A native)					negative
AT IgG to antigen ANA-Ro-52					negative
AT IgG to antigen SS-B					negative
AT IgG to antigen Scl-70					negative
AT IgG to antigen PM-Scl					negative
AT IgG to antigen CENP B					negative
AT IgG to antigen Jo-1					negative

Table 5: Dynamics of autoantibodies.

A single slight increase in IgG4 was recorded.

Data from instrumental research methods

Fibro gastroduodenoscopy performed on August 16, 2021: endoscopic signs of atrophic gastritis in the body and antrum.

Fibrocolonoscopy dated 13.10.2022

The colon is examined from the anus to the terminal ileum. The mucosa of the terminal ileum is pink and clean. The anus is closed. The tone of the colon is significantly reduced in all sections, the folds are flattened, and the distance between the haustra is more than 4 cm. The lumen of the colon is dilated due to hypotony. The mucous membrane of the sigmoid and rectum is hyperemic, edematous, and the vascular pattern is blurred. There are multiple hypertrophied submucosal lymphoid follicles measuring up to 0.2 cm from the proximal part of the sigmoid to the rectal ampulla. Conclusion: severe hypotension of the large intestine. Endoscopic signs of catarrhal proctosigmoiditis.

MR cholangiography 29.04.2022

Liver: right lobe 17.6x11.9 cm, left lobe 12.9x11.9 cm, diffuse-heterogeneous structure, intrahepatic bile ducts are not dilated. Portal vein up to 0.95 cm in diameter. Gallbladder: with a kink in the neck area, measuring 5.7x2.2x1.6 cm, with a non-thickened wall, heterogeneous contents, and the presence of The anterior wall of the parietal section has an iso-intense signal, up to 0.3x0.1 cm in size. The choledoch has filling defects. The pancreas is of normal size, with a diffuse and heterogeneous structure, and contains small cysts. The pancreatic duct is not dilated and is twisted. The spleen is not enlarged, measuring 12x5.5 cm, and has a clear and even contour. In the area of the posterior contour of the left liver lobe, a lymph node is detected, measuring up to 0.9x0.8 cm, and closely located lymph nodes are detected in the paraaortic region, measuring up to 0.9x0.7 cm. Conclusion: signs of hepatomegaly, fatty hepatosis, DGB, and a gallbladder polyp. Diffusely heterogeneous structure of the pancreas. Choledocholithiasis? MR signs of lymphadenopathy.

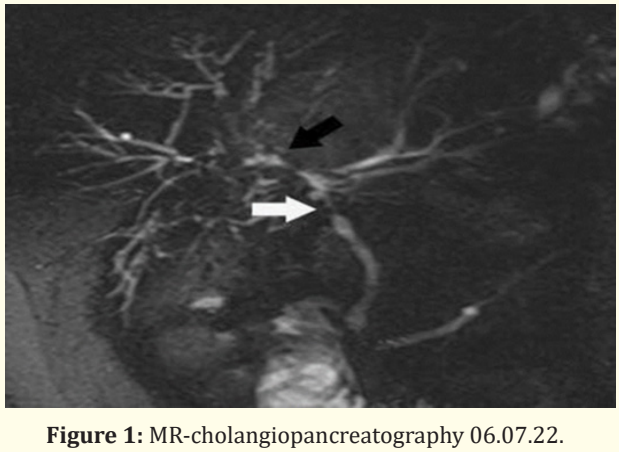

Figure 1: MR-cholangiopancreatography 06.07.22.

MR cholangiography 06.07.2022

The gallbladder is of normal size with kinks in the body and neck. A single round-shaped filling defect with a diameter of up to 3 mm (a stone?) is detected in the lumen of the neck. The intrahepatic bile ducts are not dilated. The left and right hepatic ducts are up to 4 mm in diameter. The common hepatic duct is up to 5 mm in diameter, with single round-shaped filling defects up to 3 mm in diameter (calculi?). The pancreatic duct is not dilated to 2 mm and is twisted. The choledoch is 6 mm in diameter, with single filling defects up to 3 mm in diameter. Conclusion: MRI signs of single filling defects in the lumen of the gallbladder neck, common hepatic duct, and choledoch (calculi?), as well as bends in the body and neck of the gallbladder.

According to MR-cholangiopancreatography, lymphadenopathy was diagnosed in the paraaortic region and in the posterior contour of the left liver lobe. Defects of up to 3 mm in the choledochus, the lumen of the gallbladder neck, the common hepatic duct, and the curvature of the pancreatic duct were described.

Given the immune-inflammatory syndrome, multiple lymphadenopathy, signs of cholangitis with severe cholestasis, a single slight increase in IgG4, and hepatosplenomegaly, the following diagnosis was made.

IgG4-associated cholangitis involving the extrahepatic bile ducts. Pancreatic cysts. Hepatosplenomegaly. Lymphadenopathy of the abdominal, retroperitoneal, and posterior cervical lymph nodes

Since 22.07.2023, the patient has been receiving the following treatment: prednisolone 50 mg per os, ursodeoxycholic acid 500 mg x 3 times a day, and omeprazole 20 mg x 2 times a day.

The patient's condition improved after treatment with prednisolone. According to the results of the examination, 1.5 months after the start of GCS therapy, the cholestasis gradually regressed. At the time of the second examination, the alkaline phosphatase level increased to 3 normal values, and the GGT level increased to 4-5 normal values. No organic pathology was detected using instrumental methods of examination.

CT of the abdominal cavity from 08.09.2022

Liver: contours are smooth, clear, structure is homogeneous, intra- and extrahepatic bile ducts are not dilated. Choledoch up to 4 mm. The gallbladder is of normal size, the walls are not thickened, the contours are smooth, clear, the contents are homogeneous. No calculi were found in the lumen of the gallbladder. The portal and splenic veins are not dilated.

The spleen is of normal shape and size, the contours are smooth and clear, and the structure and density of the parenchyma are not altered. The pancreas is not enlarged, the structure is homogeneous, the density is not altered, and the contours are smooth and clear. The pancreatic duct is not obstructed or dilated. The abdominal and retroperitoneal lymph nodes are not enlarged. No free fluid is detected. Conclusion: no organic pathology is identified.

Fibrocolonoscopy 04.08.2022

The rectum, sigmoid colon, descending colon, transverse colon, and ascending colon were examined up to the dome of the cecum. The mucosa is moderately hyperemic, and the vessels are injected. No organic pathology was detected.

Thus, we can see the effectiveness of glucocorticosteroid therapy: there is no cholangitis according to CT, and there are no filling defects in the choledochus, common hepatic duct, or gallbladder neck. The diagnosis of IgG4-associated cholangitis has been confirmed.

IgG4-associated sclerosing cholangitis (IgG4-SC) is one of the manifestations of IgG4-associated disease. It is a specific form of sclerosing cholangitis characterized by elevated serum IgG4 levels, infiltration of IgG4-positive plasma cells in the bile ducts, fibrotic changes in the ducts, and a positive response to glucocorticosteroid therapy.

Conclusion

Timely diagnosis of IgG4-SC can have important clinical and prognostic implications. The medical history of a 48-year-old patient confirms the difficulties in early diagnosis of the disease. Lymphadenopathy, immune-inflammatory syndrome, cholestasis, and filling defects in the bile ducts and the neck of the gallbladder mimicked cholangiocellular carcinoma. The titer of IgG4 antibodies was low, slightly above the normal range, and there was only a single increase in the titer. The effect of the ex juvantibus administration of prednisolone confirmed the diagnosis of an autoimmune disease. Therefore, the delayed administration of glucocorticosteroids leads to a lack of clinical effectiveness and the development of severe complications. In patients with suspected primary sclerosing cholangitis or cholangiocellular carcinoma, it is advisable to perform a timely differential diagnosis with IgG4-SC, as early administration of glucocorticosteroids can slow down the progression of the disease.

Bibliography

1. Della-Torre E, Rigamonti E, Perugino C, et al. B lymphocytes directly contribute to tissue fibrosis in patients with IgG4 -related disease. J Allergy Clin Immunol 2020;145:968-981.e14. doi:10.1016/j. jaci.2019.07.004.

2. Della-Torre E, Feeney E, Deshpande V, et al. B-cell depletion attenuates serological biomarkers of fibrosis and myofibroblast activation in IgG4-related disease. Ann Rheum Dis 2015;74:2236- 43. doi:10.1136/annrheumdis-2014-205799.

3. Mattoo H, Mahajan VS, Maehara T, et al. Clonal expansion of CD4(+) cytotoxic T lymphocytes in patients with IgG4-related disease. J Allergy Clin Immunol 2016;138:825-38. doi:10.1016/j. jaci.2015.12.1330.

4. Hao M, Liu M, Fan G, Yang X, Li J. Diagnostic value of serum IgG4 for igg4-Related Disease: A PRISMA-compliant systematic review and Meta-analysis [Baltimore]. Medicine (Baltimore) 2016;95:e3785. doi:10.1097/MD.0000000000003785.

5. Della-Torre E, Lanzillotta M, Doglioni C. Immunology of IgG4-related disease. Clin Exp Immunol 2015;181:191-206. doi:10.1111/ cei.12641.

6. Ebbo M, Grados A, Bernit E, et al. Pathologies Associated with Serum IgG4 Elevation. Int J Rheumatol 2012; 2012:602809. doi:10.1155/2012/602809.

7. Carruthers MN, Khosroshahi A, Augustin T, Deshpande V, Stone JH. The diagnostic utility of serum IgG4 concentrations in IgG4-related disease. Ann Rheum Dis 2015;74:14-8. doi:10.1136/ annrheumdis-2013-204907.

8. Kawa S, Ito T, Watanabe T, et al. The utility of serum IgG4 concentrations as a biomarker. Int J Rheumatol 2012; 2012:198314. doi:10.1155/2012/198314

9. Sarnago A, Pascual RM, Moreno MJ, Laíz B, Fuster O. IgG subclasses quantitation: Analytical performance of The Binding Site SPAPLUS® human assay and comparison with Siemens BNII® assay. Clin Biochem 2018; 51:85-9. doi:10.1016/j.clinbiochem.2017.09.004.

10. Khosroshahi A, Cheryk LA, Carruthers MN, Edwards JA, Bloch DB, Stone JH. Brief Report: spuriously low serum IgG4 concentrations caused by the prozone phenomenon in patients with IgG4-related disease. Arthritis Rheumatol 2014;66:213-7. doi:10.1002/ art.38193.

11. Yu KH, Chan TM, Tsai PH, Chen CH, Chang PY. Diagnostic Performance of Serum IgG4 Levels in Patients With IgG4-Related Disease [Baltimore]. Medicine (Baltimore) 2015;94:e1707. doi:10.1097/MD.0000000000001707.

12. Doorenspleet ME, Hubers LM, Culver EL, et al. Immunoglobulin G4(+) B-cell receptor clones distinguish immunoglobulin G 4-related disease from primary sclerosing cholangitis and biliary/pancreatic malignancies. Hepatology 2016; 64:501-7. doi:10.1002/hep.28568.

13. Chan ASY, Mudhar H, Shen SY, et al. Serum IgG2 and tissue IgG2 plasma cell elevation in orbital IgG4-related disease (IgG4-RD): Potential use in IgG4-RD assessment. Br J Ophthalmol 2017;101:1576-82. doi:10.1136/ bjophthalmol-2017-310148.

14. Hirano K, Tada M, Isayama H, Yagioka H, Sasaki T, Kogure H, et al. Long-term prognosis of autoimmune pancreatitis with and without corticosteroid treatment. Gut. 2007;56(12):1719-24. DOI: 10.1136/gut.2006.115246.

15. Stone JH, Khosroshahi A, Deshpande V, Chan JK, Heathcote JG, Aalberse R, et al. Recommendations for the nomenclature of IgG4-related disease and its individual organ system manifestations. Arthritis and rheumatism. 2012;64(10):3061-7. DOI: 10.1002/art.34593.

16. Kawa S, Okazaki K, Kamisawa T, Kubo K, Ohara H, Hasebe O, et al. Amendment of the Japanese Consensus Guidelines for Autoimmune Pancreatitis, 2013 II. Extrapancreatic lesions, differential diagnosis. Journal of gastroenterology. 2014;49(5):765-84. DOI: 10.1007/s00535- 014-0944-0.

17. Kubota K, Kamisawa T, Okazaki K, Kawa S, Hirano K, Hirooka Y, et al. Low-dose maintenance steroid treatment could reduce the relapse rate in patients with type 1 autoimmune pancreatitis: a long-term Japanese multicenter analysis of 510 patients. Journal of gastroenterology. 2017;52(8):955-64. DOI: 10.1007/s00535-016- 1302-1.

18. Lanzillotta M, Mancuso G, Della-Torre E. Advances in the diagnosis and management of IgG4 related disease. BMJ. 2020 Jun 16;369:m1067. DOI: 10.1136/bmj.m1067.